Effect of electron-phonon coupling on the thermoelectric efficiency of single-quantum-dot devices

X. Zianni
Department of Applied Sciences, Technological Educational Institution of Chalkida, 34 400 Psachna, Greece
(Received 4 February 2010; revised manuscript received 14 July 2010; published 4 October 2010)

The thermoelectric properties of single-quantum-dot (QD) devices have been studied theoretically taking into account the electron-phonon coupling in the QD. The thermoelectric transport coefficients and the thermoelectric efficiency have been calculated in the sequential tunneling regime. It is shown that the thermoelectric properties depend on temperature and on intrinsic properties of the QD: the electron energy spectrum, the phonon energy, and the electron-phonon coupling strength. Different regimes have been identified. In the weak electron-phonon coupling regime, it is explicitly shown that the interplay between quantum confinement and electron-phonon coupling determines the electron thermal conductance and the thermoelectric efficiency of the device. The figure of merit ZT decreases rapidly with increasing temperature and electron-phonon coupling strength. When the electron-phonon coupling is strong, it becomes evident that the thermoelectric coefficients and the thermoelectric efficiency depend primarily on phonons.

DOI: 10.1103/PhysRevB.82.165302 PACS number(s): 73.63.Kv, 73.23.Hk, 72.20.Pa

I. INTRODUCTION

A measure of the thermoelectric efficiency of a material is the dimensionless figure of merit $ZT \equiv S^2 \sigma T / \kappa$, where σ is the conductivity, S is the thermopower, κ is the thermal conductivity, and T is the absolute temperature. For $ZT \to \infty$, the Carnot heat engine efficiency is reached.[1,2] Solid-state materials have typically much lower ZTs. Even the best bulk thermoelectric materials have thermoelectric figure of merit $ZT < 1$. Scientific research and technology are currently oriented toward identifying materials and structures with $ZT > 1$, that will allow developing new thermoelectric devices with enhanced efficiency in order to contribute to the needs of our society for energy production.[3]

Low-dimensional structures are by principle expected to have better thermoelectric performance compared to the corresponding bulk materials due to quantum confinement.[4] Indeed, enhancement of ZT has been demonstrated in superlattices and this has initiated intensive research activity worldwide in the field of thermoelectrics in superlattices, thin films, wires, quantum-dot superlattices, and nanocomposite materials.[5–27] Nanostructures are currently at the center of scientific research in the field of thermoelectricity because they have shown significantly improved thermoelectric performance that has been attributed to the intrinsic materials properties at the nanoscale and to the related architectures.[28–35]

QDs are low-dimensional structures with three-dimensional (3D) confinement that have dimensions at the nanoscale (nanocrystals) and they are the basic units of nanocomposite materials. A QD provides a model system to study the thermoelectric properties at the nanoscale and to explore the possibilities and the limitations in achieving high values of ZT. QDs are characterized by discrete energy spectra. The discontinuous energy spectrum of a QD and the Coulomb-blockade effect introduce discontinuities in the electron conductance that explains the violation of Wiedemann-Franz law demonstrated[36,37] in this system. In the quantum regime, where the discreteness of the energy spectrum dominates, considerable blocking of the electron thermal conductance has been shown[36,38] that depends nearly exponentially on the ratio of the energy levels spacing over the thermal energy, $\Delta E / k_B T$. When the thermal conductance is low, the thermoelectric efficiency, measured by the dimensionless figure of merit ZT, is high. Giant thermopower and figure of merit have been predicted in single molecule devices[39] and molecular junctions.[40] It has been reported[41] that ZT increases very rapidly with the ratio $\Delta E / k_B T$ when the electron-phonon coupling is weak and it has been emphasized that ZT of a single-QD device is assigned much smaller values when the electron-phonon coupling is not weak. Hence, in order to predict the thermoelectric efficiency of a real QD device and to interpret experimental observations, it is very important to take into account electron-phonon coupling. The importance of inelastic effects in electronic transport at the nanoscale has been also pointed out in several recent scientific works[42–47] and it is theoretically explored here for the thermoelectric transport properties of QD devices.

We present our calculations on the thermoelectric coefficients and the thermoelectric efficiency in the sequential tunneling regime within a linear response theory. The theoretical model and the formalism developed in previous works[36,38,48,49] have been extended to include electron-phonon coupling. We concentrate on the quantum regime where the discreteness of the energy spectrum of the QD dominates and it results to high values of ZT. In this regime, deviation from the bulk behavior is expected for phonons. In bulk, phonons occupy continuous energy states in bands and they are described by their type and their wave vector. In low-dimensional structures, phonon dispersion undergoes strong modification due to quantum confinement. In QD superlattices, it has been demonstrated[50] that acoustic-phonons occupy quasioptical branches which are bands with narrow energy dispersion that are separated by energy gaps. In the case of strong 3D confinement the phonon energy spectrum is discrete.[51] Phonon effects in molecular transistors have been studied theoretically considering phonons being internal modes that correspond to vibrations of the QD for which the center of mass is at rest.[52] Vibrations directly couple to the electric charge in the QD. Koch *et al.*[53] have studied the thermopower of single-molecule devices taking into account

the coupling between electrons and vibrations. The same model for phonons has been used in Ref. 54 to study theoretically electronic transport in a carbon nanotube QD and to interpret experimental findings on the conductance.[55,56] The main parameter of the model is the electron-phonon coupling strength λ. This parameter depends on the material of the QD and the type of phonons. In Ref. 57, λ is estimated for polar semiconductor QDs and it has been shown that strong electron-phonon coupling may be responsible for the shape of the conductance resonances measured in scanning tunneling spectroscopy experiments. Raman spectra could provide information on phonon properties in QDs devices. It should be emphasized that for an accurate analysis of experimental Raman spectra, theoretical calculations should be required to distinguish phonon confinement effects on Raman spectra from alloying and strain induced effects.[58]

In the present work, electron tunneling through a level coupled to a phonon (local vibration) mode is assumed and our previous theoretical model has been extended to calculate the thermoelectric properties and efficiency of a QD transistor in the quantum regime. Due to electron-phonon coupling, electron tunneling is accompanied by changes in the number of phonons in the QD. Representative numerical data are presented for broad range of the parameters of the model. The transport coefficients and the thermoelectric performance of the single-QD device have been found to depend on temperature and on intrinsic properties of the dot: the electron-energy spectrum, the phonon energy, and the electron-phonon coupling strength. The dependence is not trivial and different regimes have been identified. Analytical formalism has been derived for the dependence of the thermoelectric efficiency of a single-QD device on quantum confinement and on the strength of the electron-phonon coupling.

The conclusions for the thermoelectric efficiency are drawn by taking into account the effects of the discrete energy spectrum of the QD and of the electron-phonon coupling. The thermal conductance is here approximated by the electron thermal conductance. The values of ZT calculated by neglecting the phonon thermal conductivity of the device provide upper limits in each regime of parameters. In order to estimate the effect of the phonon thermal conductivity, one has to take into account phonon conduction through the whole structure (electrodes, barriers, and QD) and for this reference to a real device would be needed. The importance of the phonon thermal conductivity in reducing the ZT of a single-QD device should depend very much on the properties of the materials at the tunneling barriers.[41] It should be emphasized that the structure under investigation could be proved advantageous compared to other bulk and low-dimensional structures in providing a mechanism to keep the phonon thermal contribution low. Phonon conduction could be blocked at the tunneling barriers. Then, phonon thermal conductivity would be small and ZT would be optimal. One way to achieve this would be by selecting barrier materials with low lattice thermal conductivity. Additional effects such as phonon confinement in the barriers and/or the dot and phonon scattering at the interfaces[59] would further contribute to keep the total phonon thermal conductivity low.

As in Refs 36 and 38, we concentrate on the sequential tunneling regime. Higher-order contributions such as cotunneling have not been included in the theoretical model presented here. It should be noted that cotunneling is not expected to affect our main conclusions because it dominates the low-temperature electron transport in the case of relatively large dots where the effects of finite quantum level spacing can be neglected.[60] Moreover, it has been shown both theoretically[60] and experimentally[61] that cotunneling influences the conductance and the thermopower away from the conductance peak and it is most important in the region between two conductance peaks. Here, important physical behavior is indicated near the conductance peak where the power factor, S^2GT, maximizes.

The theoretical model is presented in Sec. II and the results are presented and discussed in Sec. III where it is also been given simplified approximate formalism to interpret the physics of the numerical data. The conclusions are given in Sec. IV.

II. THEORETICAL MODEL

The single-QD device consists of a QD weakly coupled to two electron reservoirs via two tunnel barriers. The two reservoirs serve as the source and the drain leads and a third lead serves as the gate that interacts with electrons electrostatically. A continuum of electron states is assumed in the reservoirs that are occupied according to the Fermi-Dirac distribution

$$f(E-E_F)=\left[1+\exp\left(\frac{E-E_F}{k_BT}\right)\right]^{-1}, \tag{2.1}$$

where the Fermi energy, E_F, in the reservoirs is measured relative to the local conduction band bottom. Across the two leads there are applied a bias voltage V and a temperature difference ΔT. It is assumed that the left reservoir is at lower energy under positive bias.

The QD is characterized by discrete electron energy levels E_p $(p=1,2,\ldots)$. Degeneracies can be included by multiple counting of the levels.[36,38] In the absence of coupling to the leads, the states of the QD are denoted by (N,q) where N is the number of additional electrons in the QD and q is the number of excited phonons. The energy of the QD in a state (N,q) with respect to the conduction band bottom of the left reservoir, can be written[41,48,49] as

$$E_q^N=\sum_p n_pE_p+U(N)+\eta eVN+\hbar\omega\left(q+\tfrac{1}{2}\right), \tag{2.2}$$

where n_p is the electron occupation number, η is the part of the bias voltage V that drops across the QD and $\hbar\omega$ is the phonon energy. The electrostatic energy $U(N)$ of the dot with charge $Q=-Ne$ is

$$U(N)=(Ne)^2/2C-N\varphi_{ext}, \tag{2.3}$$

where C is the effective capacitance between the QD and the reservoir leads and ϕ_{ext} is the contribution of external charges and it is externally controlled via the gate bias.[48]

Phonons are internal modes that correspond to vibrations of the QD for which the center of mass is at rest. Vibrations directly couple with the electric charge in the QD. The

electron-phonon coupling term can be eliminated by a canonical transformation of the Hamiltonian.[52] This yields a renormalization of the parameters E_p, U. In the weak-coupling regime between the QD and the reservoir leads, electron tunneling introduces transitions between the states of the QD: $(N,q)\rightarrow(N',q')$.

The total rate for a transition $(N,q)\rightarrow(N',q')$ is denoted by $W^{N\rightarrow N'}_{q\rightarrow q'}$. First-order perturbation theory yields sequential tunneling processes $(N,q)\rightarrow(N\pm1,q')$ with total rates

$$W^{N\rightarrow N+1}_{q\rightarrow q'} = \sum_{a=L,R} f_a[E^{N+1}_{q'} - E^N_q]\Gamma^{N\rightarrow N+1}_{q\rightarrow q';a}, \tag{2.4}$$

$$W^{N\rightarrow N-1}_{q\rightarrow q'} = \sum_{a=L,R} \{1 - f_a[E^N_q - E^{N-1}_{q'}]\}\Gamma^{N\rightarrow N-1}_{q\rightarrow q';a}, \tag{2.5}$$

where the summations are over the left (L) and right (R) reservoir leads. The bare transition rates are obtained by Fermi's golden rule

$$\Gamma^{N\rightarrow N\pm1}_{q\rightarrow q';a} = \frac{2\pi}{\hbar}\rho_a\gamma^p_a|M^{N\rightarrow N\pm1}_{q\rightarrow q';a}|^2, \tag{2.6}$$

where ρ_a is the density of states in the lead α and γ^a_p is the tunnel rate from level p to reservoir α. The density of states is here assumed independent of the transition energies and the charge of the dot.

The matrix elements $M^{N\rightarrow N\pm1}_{q\rightarrow q';a}$ are[52,53]

$$M^{N\rightarrow N-1}_{q\rightarrow q';a} = (q_1!/q_2!)^{1/2}\lambda^{q_2-q_1}e^{-\lambda^2/2}L^{q_2-q_1}_{q_1}(\lambda^2) \times \begin{cases} (-1)^{q'-q} & \text{for } q'\geq q \\ 1 & \text{for } q'<q \end{cases}, \tag{2.7}$$

where $q_1=\min\{q,q'\}$ and $q_2=\max\{q,q'\}$. The parameter λ is the electron-phonon coupling parameter and can assume values both smaller and larger than 1. The functions $L^n_m(x)$ denote the generalized Laguerre polynomials. There is no dependence on the lead index α. The corresponding matrix element for a transition $N\rightarrow N+1$ can be obtained by using

$$M^{N\rightarrow N-1}_{q\rightarrow q';a} = M^{N\rightarrow N+1}_{q'\rightarrow q;a}. \tag{2.8}$$

The stationary current through the left reservoir is equal to the total current and it is given by

$$I = -e\sum_{p=1}^{\infty}\sum_{\{n_i\}}\sum_{q,q'} P_q(\{n_i\})[W^{N\rightarrow N+1}_{q\rightarrow q';L} - W^{N\rightarrow N-1}_{q\rightarrow q';L}], \tag{2.9}$$

where $P_q(\{n_i\})$ is the nonequilibrium probability distribution for an electron occupation configuration $\{n_i\}$ in the presence of q phonons. $P_q(\{n_i\})$ is a stationary solution of the kinetic equation.

$$\frac{\partial}{\partial t}P_q(\{n_i\}) = 0 = \sum_p\sum_{q'}[P_{q'}(n_1,\ldots,n_{p-1},0,n_{p+1},\ldots)\delta_{n_p,1}W^{N-1\rightarrow N}_{q'\rightarrow q} + P_{q'}(n_1,\ldots,n_{p-1},1,n_{p+1},\ldots)\delta_{n_p,0}W^{N+1\rightarrow N}_{q'\rightarrow q} - P_q(\{n_i\})\delta_{n_p,0}W^{N\rightarrow N+1}_{q\rightarrow q'} - P_q(\{n_i\})\delta_{n_p,1}W^{N\rightarrow N-1}_{q\rightarrow q'}]. \tag{2.10}$$

The kinetic equation has been solved in the linear regime similarly as in Refs. 48 and 49. Linearized expressions have been obtained for the electric current and the heat flux that lead to the following expressions for the conductance, G, the thermopower, S and the thermal conductance, κ

$$G = L^{(0)}, \tag{2.11}$$

$$S = -\frac{1}{eT}(L^{(0)})^{-1}L^{(1)}, \tag{2.12}$$

$$\kappa = \frac{1}{e^2T}[L^{(2)} - L^{(1)}(L^{(0)})^{-1}L^{(1)}], \tag{2.13}$$

$$L^{(\alpha)} = \frac{e^2}{k_BT}\sum_{p=1}^{\infty}\sum_{N=1}^{\infty}\sum_{q,q'}\frac{\gamma^L_p\gamma^R_p}{\gamma^L_p+\gamma^R_p}M^{N,N-1}_{q,q'}(\varepsilon-E_F)^{(\alpha)} \times P^q_{eq}(N)F_{eq}(E_p/N)[1-f(\varepsilon-E_F)], \tag{2.14}$$

where $\varepsilon = E_p + U(N) - U(N-1) + \hbar\omega(q-q')$. $P^q_{eq}(N)$ is the probability that the QD is in the state (N,q) in equilibrium. It holds: $P^q_{eq}(N) = e^{-\hbar\omega q/k_BT}(1-e^{-\hbar\omega/k_BT})P_{eq}(N)$. $F_{eq}(E_p/N)$ is the conditional probability in equilibrium that level p is occupied given that the QD contains N electrons. The above equilibrium probabilities are, respectively, defined[48] as

$$P_{eq}(N) = \sum_{\{n_i\}} P_{eq}(\{n_i\})\delta_{N,\sum_i n_i}, \tag{2.15}$$

$$F_{eq}(E_p/N) = \frac{1}{P_{eq}(N)}\sum_{\{n_i\}} P_{eq}(\{n_i\})\delta_{n_{p,1}}\delta_{N,\sum_i n_i}. \tag{2.16}$$

$P_{eq}(\{n_i\})$ is the Gibbs distribution in the grand canonical ensemble

$$P_{eq}(\{n_i\}) = Z^{-1}\exp\left[-\frac{1}{k_BT}\left(\sum_{i=1}^{\infty}E_in_i + U(N) - NE_F\right)\right], \tag{2.17}$$

where $N\equiv\sum_i n_i$ and Z is the partition function

$$Z = \sum_{\{n_i\}}\exp\left[-\frac{1}{k_BT}\left(\sum_{i=1}^{\infty}E_in_i + U(N) - NE_F\right)\right]. \tag{2.18}$$

A measure of the thermoelectric energy conversion efficiency is the dimensionless figure of merit ZT

$$ZT = \frac{S^2G}{\kappa_e+\kappa_{ph}}T. \tag{2.19}$$

The denominator of the above equation is the thermal conductance that consists of the electron part, κ_e, and the phonon (lattice) part, κ_{ph}. The phonon contribution originates from phonon transport through the device and it has been

neglected for the reasons discussed in Sec. I. In the calculations of the electron thermal conductance κ_e the electron energy spectrum of the QD and the electron-phonon coupling are taken into account. To simplify the notation, the electron thermal conductance is denoted by the symbol κ.

III. RESULTS AND DISCUSSION

In this section, we present the results of our calculations and we discuss the thereby indicated physical behavior. For this, reference is made to representative numerical results of extended calculations on the thermoelectric transport properties of single-QD devices. The plotted results are for QDs with equidistant energy spectrum and nondegenerate energy levels. The conclusions can be applied to more general cases of energy spectra by taking into account the effects of nonequidistant electron-energy spectrum and of energy degeneracies on the thermoelectric coefficients that have been studied previously.[36,38]

In the quantum regime, quantum confinement dominates and a single charging state contributes to transport. The term with $N=N_{\min}$ gives the dominant contribution to the sums over N in Eq. (2.14), where $N_{\min}$ is the integer that minimizes the absolute value of $\Delta(N)=E_N+U(N)-U(N-1)-E_F$. They are defined: $\Delta\equiv\Delta(N_{\min})$, $\Delta_p\equiv E_p-E_{N_{\min}}$, and $\Delta_{qq'}\equiv\Delta+\hbar\omega(q-q')$. Periodic Coulomb-blockade oscillations have been shown in the calculated transport coefficients when electron-phonon coupling is neglected.[36,38,48,49] The peaks of the conductance, the thermopower and the thermal conductance occur each time an extra electron enters the QD with periodicity $\Delta E_F=\Delta E+e^2/C$. Additional sawtooth short-period oscillations of the thermopower are due to the discreteness of the energy spectrum.

The electron-phonon coupling parameter λ can be estimated by the ratio $\Delta r/\lambda_{vib}$, where Δr is the shift of the phonon potential curve due to the additional electron on the QD and λ_{vib} is the harmonic oscillator length corresponding to vibrations.[53] Since, there is no direct connection between Δr and λ_{vib}, parameter λ can assume values both smaller and larger than 1.[53] The values of λ, of the relevant confinement energy ΔE and of the phonon energy $\hbar\omega$ should be known in order to estimate the energy conversion efficiency of QD device. (For instance for carbon nanotube QDs estimated[54] parameters values are: $\Delta E=30$ meV, $\lambda=1.6$, and $\hbar\omega=11.5$ meV.) The thermoelectric coefficients depend on the magnitude of λ. We first discuss the calculated behavior for values of λ smaller than unity. This regime is referred to as "weak electron-phonon coupling regime." Then, we discuss the obtained behavior for values of λ comparable to or greater than unity. This regime is referred to as "strong electron-phonon coupling regime."

A. Weak electron-phonon coupling regime

For small values of λ, the electron conductance G is practically not affected by phonons and it holds: $G\simeq G_o\equiv G|_{\lambda=0}$. G is plotted in Fig. 1 for $\lambda=0.2$. When $\Delta E\gg k_BT$, the

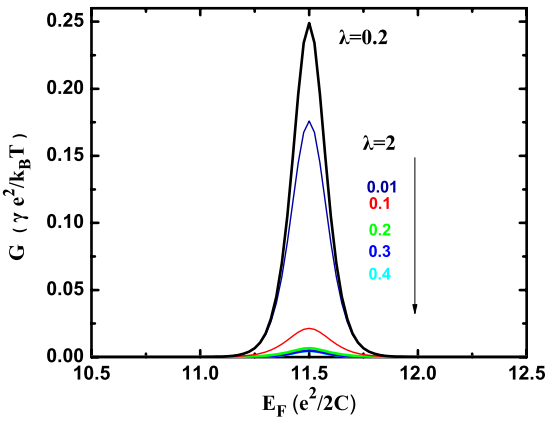

FIG. 1. (Color online) A period of the conductance, G, versus Fermi energy, E_F, for $\Delta E=0.5\ e^2/2C$ and $k_BT=0.05\ e^2/2C$ (i) for $\lambda=0.2$ (thick solid line) where the data for the various phonon frequencies are not distinguishable on the scale of the figure, and (ii) for $\lambda=2$ (solid lines) and phonon energies $\hbar\omega=0.01,0.1,0.2,0.3,0.4\ e^2/2C$.

Coulomb-blockade oscillations of G can be interpreted by the formula.[36,48]

$$G\simeq G_o=\frac{e^2}{k_BT}\gamma\frac{1}{4\cosh^2(\Delta/2k_BT)}, \tag{3.1}$$

where $\gamma\equiv\frac{\gamma^L\gamma^R}{\gamma^L+\gamma^R}$.

The electron conductance does not depend on phonons because electron tunneling does not cause any significant phonon transitions for weak coupling. Diagonal transitions, such as $(N,q)\rightarrow(N\pm1,q)$ give the dominant contribution to G except for very small phonon energies. Phonon transitions occur when phonon energies are very small and in this case off-diagonal terms contribute to G. The total conductance can still be interpreted by Eq. (3.1).

The thermopower S does not depend on phonon energy and is nearly the same as that for $\lambda=0$, i.e., $S\simeq S_o\equiv S|_{\lambda=0}$ (Fig. 2). The steps in the Coulomb oscillations are due to the electron activation-energy spectrum of the QD and they are distinguishable at low temperatures.[49] In the weak-coupling

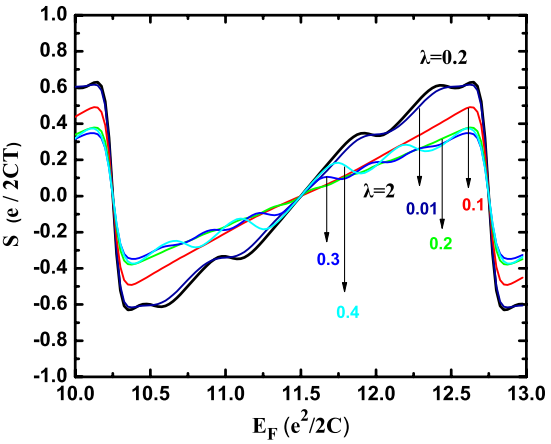

FIG. 2. (Color online) A period of the thermopower, S, versus Fermi energy, E_F, for parameters and lines format as in Fig. 1.

regime, steps due to phonon-energy states are not observable because their height is small.

The electron thermal conductance κ is enhanced due to electron-phonon coupling even when the coupling is weak. The enhancement depends on phonon energy. This is shown in Fig. 3, where κ is plotted for $\lambda=0.2$ for various phonon energies together with $\kappa_0 \equiv \kappa|_{\lambda=0}$. It has been previously shown[36,38] that κ_0 is highly limited by the discrete energy spectrum of the QD. κ_0 increases with temperature due to thermal broadening of the transition probability. Its magnitude is determined by the interplay of the thermal energy and the confinement energy. It increases nearly exponentially with the ratio of $k_BT/\Delta E$. The enhancement of κ relative to κ_0 is due to the broadening of the transition probability by additional possible transitions $(N,q)\rightarrow(N\pm1,q')$ due to electron-phonon coupling. Analysis of our numerical data has indicated that κ can be approximated by the sum of two contributions: $\kappa_{\Delta E}$ that mainly depends on the electron energy spectrum of the QD and κ_{e-ph} that mainly depends on the electron-phonon coupling

$$\kappa \approx \kappa_{\Delta E} + \kappa_{e-ph}, \tag{3.2}$$

$$\kappa_{\Delta E} = k_B\gamma\left(\frac{\Delta E}{k_BT}\right)^2 e^{-\Delta E/k_BT}\sum_{q,q'} F_{qq'} \times \left\{(\zeta_p^{qq'}e^{\Delta_{qq'}/k_BT} + \zeta_n^{qq'}) - e^{-\Delta E/k_BT}(\zeta_p^{qq'}e^{\Delta_{qq'}/k_BT} - \zeta_n^{qq'})\frac{\sum_{m,m'} F_{mm'}(\zeta_p^{mm'}e^{\Delta_{mm'}/k_BT} - \zeta_n^{mm'})}{\sum_{m,m'} G_{mm'}}\right\}, \tag{3.3}$$

$$\kappa_{e-ph} = k_B\gamma\left(\frac{1}{k_BT}\right)^2\sum_{q,q'} G_{qq'}\Delta_{qq'}(\Delta_{qq'} - \langle\Delta_{qq'}\rangle), \tag{3.4}$$

where

$$\zeta_p^{qq'} = \begin{cases} 1 & \text{for } \Delta E \gg k_BT \\ \dfrac{1}{1+e^{(\Delta_p+\Delta_{qq'})/k_BT}} & \text{elsewhere} \end{cases}, \tag{3.5}$$

$$\zeta_n^{qq'} = \begin{cases} 1 & \text{for } \Delta E \gg k_BT \\ \dfrac{e^{(\Delta_p+\Delta_{qq'})/k_BT}}{1+e^{(\Delta_p+\Delta_{qq'})/k_BT}} & \text{elsewhere} \end{cases}, \tag{3.6}$$

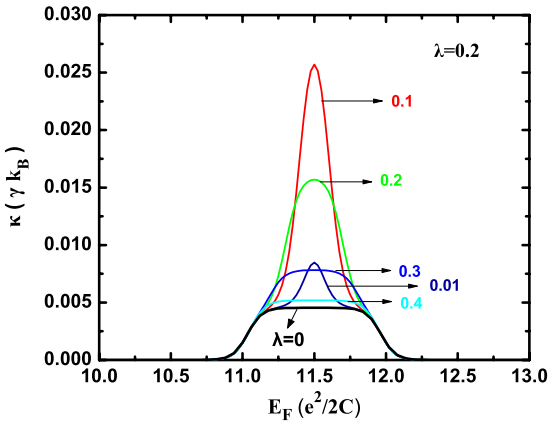

FIG. 3. (Color online) A period of the thermal conductance, κ, versus Fermi energy, E_F, for $\lambda=0.2$ for phonon energies $\hbar\omega=0.01,0.1,0.2,0.3,0.4$ $e^2/2C$ for $\Delta E=0.5$ $e^2/2C$ and $k_BT=0.05$ $e^2/2C$. κ_0 for $\lambda=0$ (thick solid line) is also shown for reference.

$$F_{qq'} = e^{-\hbar\omega q/k_BT}(1-e^{-\hbar\omega/k_BT})\frac{1}{1+e^{\Delta/k_BT}}M_{qq'}^2, \tag{3.7}$$

$$G_{qq'} = F_{qq'}\left(\zeta_p^{qq'}e^{(-\Delta E+\Delta_{qq'})/k_BT} + \frac{e^{\Delta_{qq'}/k_BT}}{1+e^{\Delta_{qq'}/k_BT}} + \zeta_n^{qq'}e^{-\Delta E/k_BT}\right), \tag{3.8}$$

and

$$\langle\Delta_{qq'}\rangle \equiv \frac{\sum_{q,q'} G_{qq'}\Delta_{qq'}}{\sum_{q,q'} G_{qq'}}. \tag{3.9}$$

The first term of Eq. (3.2) can be approximated by κ_0: $\kappa_{\Delta E}\approx\kappa_0$. As in G, diagonal transitions also dominate in this term of κ. The enhancement of κ relative to κ_0 (Figs. 3 and 4) originates from the second term, κ_{e-ph}. This term depends on the deviation of $\Delta_{qq'}$ for the phonon transitions $q\rightarrow q'$ from $\langle\Delta_{qq'}\rangle$ [Eq. (3.9)]. $\langle\Delta_{qq'}\rangle$ can be interpreted as an average of the sequential tunneling transition energy on the conductance channels. Due to electron-phonon coupling the probable transitions are broadened around the average tunneling resonance. The additional contribution to the electron thermal conductance is the sum of all deviations of $\Delta_{qq'}$ from the average $\langle\Delta_{qq'}\rangle$. This is zero for the diagonal terms. The phonon transitions offer extra channels for thermal conduction resulting to an enhancement of κ that maximizes at certain phonon energy (Fig. 4).

ZT is plotted in Fig. 5 together with ZT_0 $(\equiv ZT|_{\lambda=0})$ for comparison. In quantum regime, ZT_0 has been predicted to assume very high values due to the discrete energy spectrum of the QD as interpreted by the following approximate expression:[41]

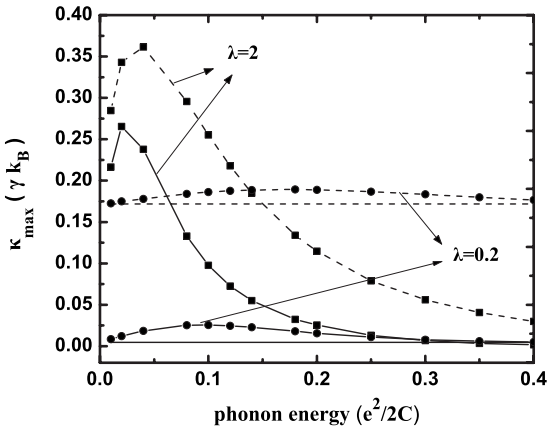

FIG. 4. κ_{max} versus the phonon energy ($\hbar\omega$) for $\lambda=0.2$ (dots) and $\lambda=2$ (squares) at $k_BT=0.05$ $e^2/2C$ (solid eye guide line) and $k_BT=0.1$ $e^2/2C$ (dashed eye guide line). The horizontal straight lines are for $\lambda=0$ and are shown for reference. It is $\Delta E=0.5$ $e^2/2C$.

$$ZT|_{\lambda=0} = \left(\frac{\Delta}{\Delta E}\right)^2 e^{\Delta E/k_BT}\frac{[1+4\cosh^2(\Delta/2k_BT)e^{-\Delta E/k_BT}]}{4\cosh^2(\Delta/2k_BT)} \times\left[1-4\left(\frac{\Delta E}{\Delta}\right)\sinh(\Delta/k_BT)e^{-\Delta E/k_BT} + 4\left(\frac{\Delta E}{\Delta}\right)^2\sinh^2(\Delta/k_BT)e^{-2\Delta E/k_BT}\right]. \quad (3.10)$$

Equation (3.10) has a simple form and it can be used to estimate ZT when quantum confinement dominates. For $\Delta E \gg k_BT$, this expression can be further simplified by neglecting the second and third terms in the bracket. For QDs with $\Delta E \geq k_BT$, nonequidistant energy spectra and degeneracies, a more accurate analytical expression for ZT, can be obtained by replacing in the definition of ZT the analytical expressions given in Ref. 38 for the transport coefficients G, S, and κ.

Calculated data for ZT are plotted in Fig. 5 at low-thermal energy, $k_BT=0.05$ $e^2/2C$. It can be seen that even at low temperatures, for some phonon energies, ZT can be significantly lower than the value expected by quantum confinement, ZT_0. The reason for this can be understood by recalling the definition of ZT. The nominator of Eq. (2.9) is the power factor, S^2GT, that is a function of G and S and it is nearly independent of the phonon parameters: $S^2GT \approx S_o^2G_oT$. Hence, the decrease in ZT relative to ZT_0 is solely due to the enhancement of κ relative to κ_0 due to the coupling of tunneling electrons with phonons. It should be emphasized that although this decrease, ZT still assumes high values. With increasing temperature, the difference between ZT and ZT_0 becomes smaller and less dependent on phonon energy. It has been found that for electrons tunneling through discrete transition energy levels of isolated QDs, ZT is more importantly limited by increasing thermal energy than by electron-phonon coupling.

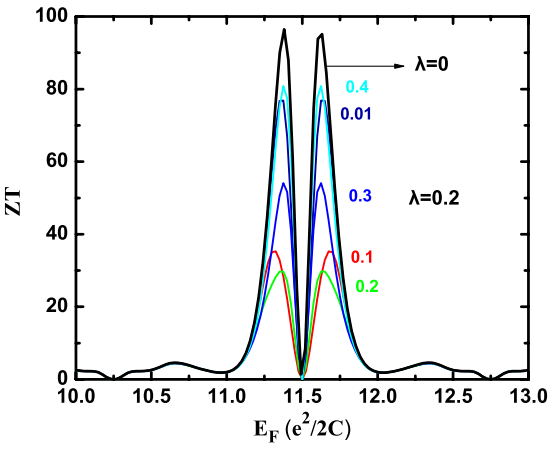

FIG. 5. (Color online) The figure of merit ZT for $\lambda=0.2$ for phonon energies $\hbar\omega=0.01,0.1,0.2,0.3,0.4$ $e^2/2C$ at $k_BT=0.05$ $e^2/2C$. The thick solid curve is ZT_0.

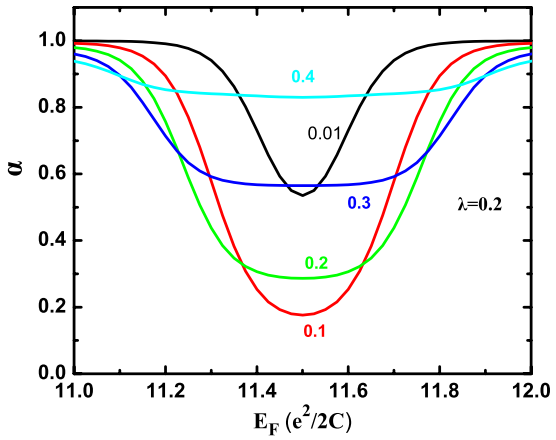

FIG. 6. (Color online) Coefficient α for $\lambda=0.2$, $\hbar\omega=0.01,0.1,0.2,0.3,0.4$ $e^2/2C$ for $\Delta E=0.5$ $e^2/2C$ and $k_BT=0.05$ $e^2/2C$.

A simple approximate expression has been deduced that relates the figure of merit, ZT to $ZT_0 \equiv ZT|_{\lambda=0}$

$$ZT \approx aZT_0, \quad (3.11)$$

$$a = \left(1+\frac{\kappa_{e-ph}}{\kappa_{\Delta E}}\right)^{-1}. \quad (3.12)$$

The coefficient a measures the effect of the electron-phonon coupling on the thermoelectric efficiency of a QD device that would be ZT_0 if determined by the discrete energy spectrum of the QD. It measures the reduction in ZT relative to ZT_0 and it is plotted in Fig. 6 for various phonon energies. Equations (3.9)–(3.12) can provide estimations of optimal ZT of a single-QD device in the weak electron-phonon coupling regime when the electron-energy spectrum, the phonon energy and the electron-phonon coupling strength are known. The thereby estimated ZTs should be approached when the phonon conduction through the whole device is small.

B. Strong electron-phonon coupling regime

In the strong electron-phonon coupling regime, the conductance G is smaller than G_0 and depends on phonon energy (Fig. 1). The decrease in G_{max} with $\hbar\omega$ is explained by that the off-diagonal transitions dominate in Eqs.

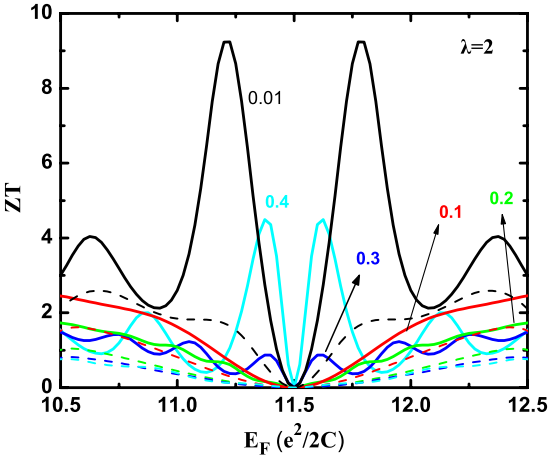

FIG. 7. (Color online) The figure of merit, ZT, for $\Delta E=0.5$ $e^2/2C$ and $k_BT=0.05$ $e^2/2C$ (solid lines) for $\lambda=2$ and $\hbar\omega=0.01,0.1,0.2,0.3,0.4$ $e^2/2C$. The dashed lines are for a higher thermal energy $k_BT=0.1$ $e^2/2C$ for the same phonon energies $\hbar\omega$.

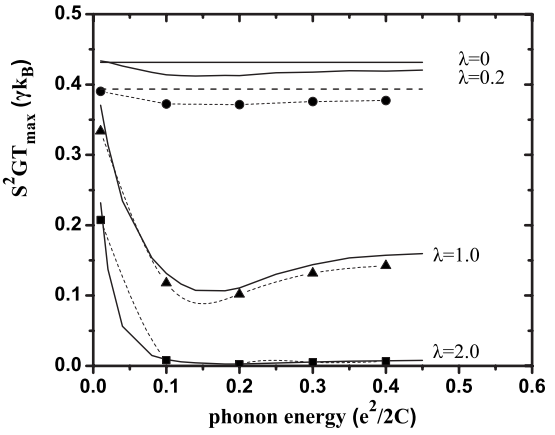

FIG. 8. $S^2GT_{\max}$ versus phonon energy for various λ at $k_BT=0.05$ $e^2/2C$ and for two cases of quantum confinement in the quantum regime: $\Delta E=0.5$ $e^2/2C$ (solid lines) ($\Delta E/k_BT=10$) and $\Delta E=0.3$ $e^2/2C$ (dashed lines) ($\Delta E/k_BT=6$).

(2.11)–(2.14), i.e., electron tunneling through the resonant transition level occurs mostly with emission and/or absorption of phonons. With increasing λ, more matrix elements $M_{qq'}$ become nonvanishing and more phonon transitions $q\rightarrow q'$ take place resulting to broadening of the transition probability and to lowering of its maximum. Increasing thermal energy makes more transitions possible and results to enhancement of G and broadening of the Coulomb peaks.

S shows additional fine structure compared to S_0 that is due to phonon transitions (Fig. 2). In the strong electron-phonon coupling regime, phononic steps are observable in S because their height is significant. The features of the phonon steps within our theoretical model are in agreement with those described in Ref. 53. The calculated power factor S^2GT decreases with phonon energy mainly due to the corresponding decrease in G.

In the quantum regime and for strong electron-phonon coupling, the thermal conductance κ may be significantly higher than κ_0. This enhancement also depends on phonon energy (Fig. 3). The enhancement of κ is due to the dominant off-diagonal phonon transitions. The off-diagonal transitions correspond to additional channels of thermal conduction that are provided by the phonon transitions upon electron tunneling. In this regime it holds that

$$\kappa \approx \kappa_{e-ph}. \tag{3.13}$$

This relation reveals the dominant role of the electron-phonon coupling in determining the thermal conductance and that the amount of electron quantum confinement in the QD plays a secondary role in this regime.

The decrease in the power factor and the increase in the thermal conductance result in significant reduction in ZT relative to ZT_0 and $ZT_{small\ \lambda}$. It is concluded that ZT of a single-QD device can be significantly limited when the electron-phonon coupling within the QD is strong. This can be clearly seen by comparing the data plotted in Figs. 5 and 7 that correspond to two devices of QDs in the quantum regime with the same amount of confinement and with different strengths of electron-phonon coupling. The data in Fig. 5 are for weak coupling ($\lambda=0.2$) and the data in Fig. 7 are for strong coupling ($\lambda=2$). The ZT values of the second device are more than one order of magnitude lower than the ZT values of the first device. The difference between the values of ZT in the two coupling regimes becomes smaller at higher temperatures. In the strong-coupling regime, ZT has been found to decrease rapidly with increasing temperature and it typically assumes values smaller than 1. In Fig. 7, it can be noticed that ZT decreases first with increasing with phonon energy $\hbar\omega$ and then it increases again. The decrease in ZT is explained by the decrease in G with $\hbar\omega$ whereas the increase is due to the decrease in κ with $\hbar\omega$.

An overview of the results on the thermoelectric performance as a function of the main parameters of the model is presented in order to make apparent the different regimes that have been identified. The maximum of the power factor $S^2GT_{\max}$ and the figure of merit at this maximum, ZT^* are plotted in Figs. 8–10 versus the phonon energy for various electron-phonon coupling strengths. Data are plotted for four values of the ratio $\Delta E/k_BT$ to show the effect of the interplay between quantum confinement and thermal energy. High ZTs are predicted for all phonon energies for small λ (weak electron-phonon coupling) and big values of $\Delta E/k_BT$. In this regime, QDs with smaller amount of confinement (i.e., smaller ΔE) are predicted to have lower ZT. In Fig. 9, it can be seen that ZT^* decreases with increasing λ. It has a minimum at some phonon energy. In the strong-coupling regime, this minimum is weakly dependent on ΔE. By comparing the data in Figs. 9 and 10, it can be seen that ZT is highly reduced by increasing temperature for all strengths of electron-phonon coupling.

IV. CONCLUSIONS

The effect of the electron-phonon coupling on the thermoelectric properties of single QD devices has been investigated. It has been shown that the high thermoelectric efficiency that has been previously predicted for electrons

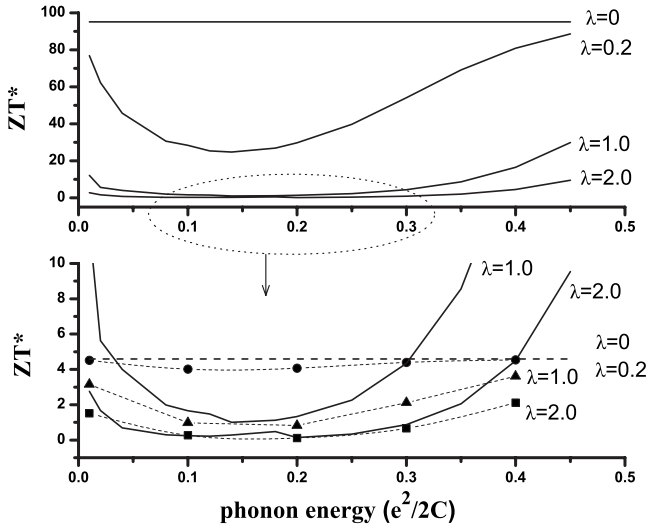

FIG. 9. ZT^* (ZT for S^2GT_{max}) versus phonon energy for parameters as in Fig. 8. The lower panel is an enlargement of the upper part for values of ZT^* up to 10.

tunneling through the discrete energy levels of the QD persists when the coupling is weak. ZT can be considerably limited when the electron-phonon coupling is not small. In the strong coupling regime, ZT typically assumes values smaller than 1 and it is mainly determined by phonon parameters.

The hereby predicted efficiencies are optimal for minimized phonon conductance through the device. It seems likely that optimal ZT could be achieved in single QD devices by exploiting that the structure is nonhomogeneous and that the active part is the material of the QD. It would be particularly challenging to design the structure and to select the materials of the tunneling barriers so that phonon conduction through the device is minimized.

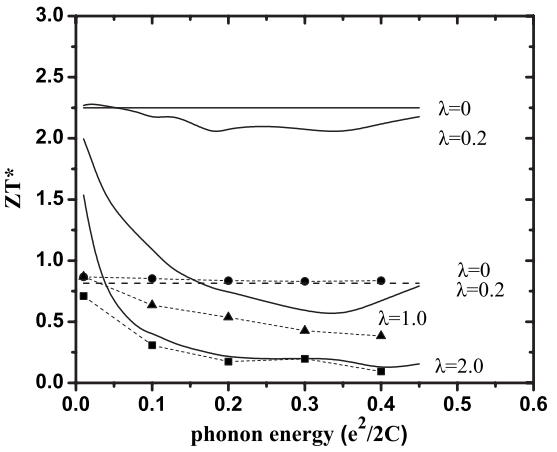

FIG. 10. ZT^* as in Fig. 9 at a higher thermal energy $k_BT=0.1$ $e^2/2C$. $\Delta E=0.5$ $e^2/2C$ (solid lines) ($\Delta E/k_BT=5$) and $\Delta E=0.3$ $e^2/2C$ (dashed lines) ($\Delta E/k_BT=3$).

Finally, it should be mentioned that the present model applies when the QD is isolated and electron tunneling occurs through deltalike transition levels. Deviations are to be expected when electrons in the QD couple to the electrodes states or to other states in the surrounding materials.

[1] M. F. O'Dwyer, T. E. Humphrey, and H. Linke, Nanotechnology **17**, S338 (2006).
[2] T. E. Humphrey and H. Linke, Phys. Rev. Lett. **94**, 096601 (2005).
[3] C. B. Vining, Nature Mater. **8**, 83 (2009).
[4] M. Dresselhaus, G. Chen, M. Y. Tang, R. Yang, H. Lee, D. Wang, Z. Ren, J. Fleurial, and P. Gogna, Adv. Mater. **19**, 1043 (2007).
[5] K. Koumoto, I. Terasaki, and R. Funahashi, MRS Bull., **31**, 206 (2006).
[6] H. Boettner, G. C. Chen, and R. Venkatasubramanian, MRS Bull. **31**, 211 (2006).
[7] J. P. Heremans, Acta Physica Polonica A **108**, 609 (2005).
[8] A. Khitun, K. L. Wang, and G. Chen, Nanotechnology **11**, 327 (2000).
[9] A. V. Andreev and K. A. Matveev, Phys. Rev. Lett. **86**, 280 (2001).
[10] A. Dauscher, B. Lenoir, H. Scherrer, and T. Caillant, Recent Res. Dev. Mater. Sci. **3**, 181 (2002).
[11] H. Beyer, J. Nurnus, H. Böttner, A. Lambrecht, T. Roch, and G. Bauer, Appl. Phys. Lett. **80**, 1216 (2002).
[12] A. A. Balandin and O. Lazarenkova, Appl. Phys. Lett. **82**, 415 (2003).
[13] J. L. Liu, A. Khitun, K. L. Wang, W. L. Liu, G. Chen, Q. H. Xie, and S. G. Thomas, Phys. Rev. B **67**, 165333 (2003).
[14] J. P. Small, K. M. Perez, and P. Kim, Phys. Rev. Lett. **91**, 256801 (2003).
[15] K. Wojciechowski and J. Oblakowski, Solid State Ion. **157**, 341 (2003).
[16] D. Vashaee and A. Shakouri, Phys. Rev. Lett. **92**, 106103 (2004).
[17] R. Yang and G. Chen, Phys. Rev. B **69**, 195316 (2004).
[18] M. C. Llaguno, J. E. Fischer, A. T. Johnson, and J. Hone, Nano Lett. **4**, 45 (2004).
[19] T. C. Harman, M. P. Walsh, B. E. Laforge, and G. W. Turner, J. Electron. Mater. **34**, L19 (2005).
[20] A. Balandin, J. Nanosci. Nanotechnol. **5**, 1015 (2005).
[21] V. Sajfert, J. P. Setrajcic, S. Jacimovski, and B. Tosic, Physica E **25**, 479 (2005).
[22] Y. Bao, W. L. Liu, M. Shamsa, K. Alim, A. A. Balandin, and J. L. Liu, J. Electrochem. Soc. **152**, G432 (2005).
[23] T. Kihara, T. Harada, and N. Koshida, Jpn. J. Appl. Phys., Part 1 **44**, 4084 (2005).
[24] M. Shamsa, W. Liu, A. A. Balandin, and J. Liu, Appl. Phys. Lett. **87**, 202105 (2005).
[25] E. I. Rogacheva, S. G. Lubchenko, and M. S. Dresselhaus, Thin Solid Films **476**, 391 (2005).
[26] E. I. Rogacheva and A. A. Drozdova, J. Thermoelectr. **2**, 22 (2006).
[27] D. Ebling, A. Jacquot, M. Jägle, H. Böttner, U. Kühn, L. Kirste, Phys. Status Solidi (RRL) **1**, 238 (2007).

[28] A. J. Minnich, H. Lee, X. W. Wang, G. Joshi, M. S. Dresselhaus, Z. F. Ren, G. Chen, and D. Vashaee, Phys. Rev. B **80**, 155327 (2009).
[29] S. Ghosh, D. L. Nika, E. P. Polatikov, and A. A. Balandin, New J. Phys. **11**, 095012 (2009).
[30] S. K. Bux, R. G. Blair, P. K. Gogna, H. Lee, G. Chen, M. S. Dresselhaus, R. B. Kaner, and J. P. Fleurial, Adv. Funct. Mater. **19**, 2445 (2009).
[31] M. Zebarjadi, K. Esfarjani, A. Shakouri, J. H. Bahk, Z. X. Bian, G. H. Z. eng, J. Bowers, H. Lu, J. Zide, and A. Gossard, Appl. Phys. Lett. **94**, 202105 (2009).
[32] J. D. Koenig, M. Winkler, and H. Boettner, J. Electron. Mater. **38**, 1418 (2009).
[33] L. Shi, J. H. Zhou, P. Kim, A. Bachtold, A. Majumdar, and P. L. McEuen, J. Appl. Phys. **105**, 104306 (2009).
[34] M. S. Dresselhaus, G. Chen, Z. F. Ren, G. Dresselhaus, A. Henry, and J. P. Fleurial, JOM **61**, 86 (2009).
[35] E. S. Toberer, S. R. Brown, T. Ikeda, S. M. Kauzlarich, and G. J. Snyder, Appl. Phys. Lett. **93**, 062110 (2008).
[36] X. Zianni, Phys. Rev. B **75**, 045344 (2007).
[37] B. Kubala, J. König, and J. Pekola, Phys. Rev. Lett. **100**, 066801 (2008).
[38] X. Zianni, Phys. Rev. B **78**, 165327 (2008).
[39] C. M. Finch, V. M. Garcia-Suarez, and C. J. Lambert, Phys. Rev. B **79**, 033405 (2009).
[40] P. Murphy, S. Mukerjee, and J. Moore, Phys. Rev. B **78**, 161406(R) (2008).
[41] X. Zianni, J. Electron. Mater. **39**, 1996 (2009).
[42] S. Monturet and N. Lorente, Phys. Rev. B **78**, 035445 (2008).
[43] A. M. Kuznetsov and I. G. Medvedev, Phys. Rev. B **78**, 153403 (2008).
[44] H. Nakamura, K. Yamashita, A. R. Rocha, and S. Sanvito, Phys. Rev. B **78**, 235420 (2008).
[45] N. Vukmirović, Z. Ikonić, D. Indjin, and P. Harrison, Phys. Rev. B **76**, 245313 (2007).
[46] M. Paulsson, T. Frederiksen, H. Ueba, N. Lorente, and M. Brandbyge, Phys. Rev. Lett. **100**, 226604 (2008).
[47] R. D'Agosta and M. DiVentra, J. Phys.: Condens. Matter **20**, 374102 (2008).
[48] C. W. J. Beenakker, Phys. Rev. B **44**, 1646 (1991).
[49] C. W. J. Beenakker and A. A. M. Staring, Phys. Rev. B **46**, 9667 (1992).
[50] O. L. Lazarenkova and A. A. Balandin, Phys. Rev. B **66**, 245319 (2002).
[51] X. Zianni, P. N. Butcher, and I. Dharssi, J. Phys.: Condens. Matter **4**, L77 (1992).
[52] A. Mitra, I. Aleiner, and A. J. Millis, Phys. Rev. B **69**, 245302 (2004).
[53] J. Koch, F. von Oppen, Y. Oreg, and E. Sela, Phys. Rev. **70**, 195107 (2004).
[54] L. Siddiqui, A. W. Ghosh, and S. Datta, Phys. Rev. B **76**, 085433 (2007).
[55] B. J. LeRoy, S. G. Lemay, J. Kong, and C. Dekker, Nature (London) **432**, 371 (2004).
[56] B. J. LeRoy, J. Kong, V. K. Pahilwani, C. Dekker, and S. G. Lemay, Phys. Rev. B **72**, 075413 (2005).
[57] L. Jdira, K. Overgaag, R. Stiufiuc, B. Grandidier, C. Delerue, S. Speller, and D. Vanmaekelbergh, Phys. Rev. B **77**, 205308 (2008).
[58] O. Lazarenkova and A. A. Balandin, Superlattices Microstruct. **33**, 95 (2003).
[59] A. Khitun, A. Balandin, J. L. Liu, and K. L. Wang, J. Appl. Phys. **88**, 696 (2000); Superlattices Microstruct. **30**, 1 (2001).
[60] M. Turek and K. A. Matveev, Phys. Rev. B **65**, 115332 (2002).
[61] R. Scheibner, E. G. Novik, T. Borzenko, M. Konig, D. Reuter, A. D. Wieck, H. Buhmann, and L. W. Molenkamp, Phys. Rev. B **75**, 041301(R) (2007).